15

Methods and Models for Computer Aided Design of Wind Power Systems for EMC and Power Quality

Vladimir Belov[1], Peter Leisner[2,3], Nikolay Paldyaev[1],
Alexey Shamaev[1] and Ilja Belov[3]
[1]*Mordovian State University, 430000, Saransk,*
[2]*SP Technical Research Institute of Sweden, Box 857, 501 15 Borås,*
[3]*School of Engineering, Jönköping University, Box 1026, SE 551 11, Jönköping,*
[1]*Russia*
[2,3]*Sweden*

1. Introduction

In off-grid wind power systems (WPS) a power source generates the power which is comparable to the consumed power. Solving electromagnetic compatibility (EMC) problems in such a WPS is directly related to power quality issues. High levels of low- and high-frequency conducted emissions in a WPS worsen the quality of consumed electric power, increase power losses, and adversely affect reliability of connected appliances. The indicated problems should be addressed in the WPS design phase. Here, power quality and EMC related criteria have to be given a high rank when choosing the structure and parameters of a WPS.

The mission of this chapter is to provide grounds for practical application of both a mathematical model of WPS and a method for parametric synthesis of a WPS with specified requirements to EMC and electric power quality.

The present chapter is focused on a simulation-based spectral technique for power quality and EMC design of wind power systems including a power source or synchronous generator (G), an AC/DC/AC converter and electronic equipment with power supplies connected to a power distribution network. A block diagram of a typical WPS is shown in Fig. 1 (EMC Filters Data Book, 2001), (Grauers, 1994).

Three-phase filter 1 is connected to the generator side converter in order to suppress current harmonics caused by the rectifier circuit. An output Γ-filter placed after the AC/DC/AC converter comprises inductance L and capacitor C. It is designed for filtering emissions caused by pulse-width modulation (PWM) in the AC/DC/AC converter.

Single-phase filter 2 (shown with the dash line) is connected to the load side inverter. It protects the load from low frequency current harmonics impressed by the AC/DC/AC converter.

A synchronous generator and an AC/DC/AC converter are the key elements of a WPS. The AC/DC/AC converter is a source of low-frequency conducted emissions. They cause voltage distortions at the synchronous generator output, thereby reducing the quality of the supplied voltage and increasing active losses. The pulse-width modulation (PWM) in the

Source: Wind Power, Book edited by: S. M. Muyeen,
ISBN 978-953-7619-81-7, pp. 558, June 2010, INTECH, Croatia, downloaded from SCIYO.COM

AC/DC/AC converter is the main source of high-frequency emissions as well as single-phase non-linear loads, such as a switch mode power supply (SMPS). High-frequency emissions create EMC problems in a WPS.

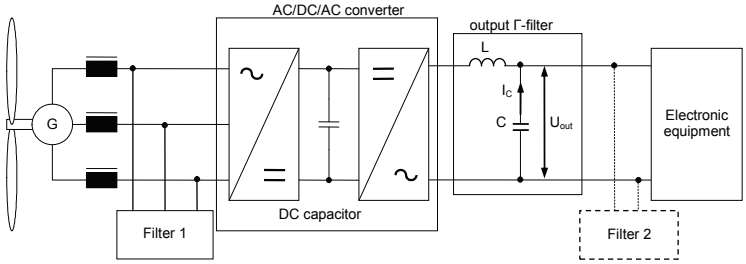

Fig. 1. Block diagram of a wind power system

The described problems of EMC and power quality can be solved on the basis of a complex approach, via designing a filtering system.

Parametric synthesis of the system of harmonic, EMC and active filters constitute an important practical task in variant design of WPS.

The task of computer aided design of the filtering system can be solved through application of the simulation-based spectral technique (Belov et al., 2006). The spectral technique utilizes multiple calculations of current and voltage spectra in the nodes of WPS during the power quality and EMC design procedure. It essentially differs from the filter design methods based on the insertion loss technique (Temes et al, 1973), since it can search for WPS frequency response and for the corresponding filter circuit given the EMC and power quality requirements for WPS. Change in the WPS frequency response during design is reflected in the spectral technique. In the proposed spectral technique, power converters and power supplies are described with complete non-linear models.

A general WPS includes a number of AC/DC/AC converters. Therefore, *a WPS modeling methodology* is developed that computes the WPS frequency response. The modeling methodology developed for a general multi-phase electric power supply system has the following features:

- Operation of all switching elements is implemented in the WPS model, for arbitrary cascade circuits including bridge converters in single-phase, three-phase and, generally, *m*-phase realizations.
- Modelling of a three-phase and, generally, an *m*-phase synchronous generator is performed according to complete equations written in *dq0* co-ordinates.

Mathematical modelling of power quality and EMC in the WPS is performed on the basis of the multi-phase bridge-element concept (B-element concept), (Belov et. al., 2009). This concept corresponds well both to the structure and to the operation principles of an AC/DC/AC converter, being efficiently tied both to the transient phenomena in electrical machines and to the PWM techniques.

Mathematical models of single- and three-phase devices in WPS are obtained as a particular case of multi-phase B-element concept. In the complete model of a WPS, the AC/DC/AC converter is represented in *m*-phase co-ordinate system, whereas electro-mechanical converters are represented in *dq0* co-ordinates, thereby contributing to modelling efficiency and validity of the results; it will be demonstrated by computational experiments,

performed for the WPS including an active filter integrated into the voltage inverter of the AC/DC/AC converter

2. Spectral technique for power quality and EMC design of wind power systems

The problem of EMC and power quality design of the WPS shown in Fig. 1 may include calculation of filter 1 and filter 2 which can be either active or harmonic filters, as well as any additional filter installed in the WPS. The steps of the simulation-based spectral technique will thus be formulated on the example of a general filter.

Calculation of the filter includes an optimization procedure. Objective function and constraints are defined based on application reasons. For example, the total reactive power Q of the filter capacitors defines the volumetric dimensions of the filter, which in some applications is an important design criterion. Minimization of the total reactive power of filter capacitors can be performed for a passive harmonic filter (Belov et al., 2006). Active and hybrid filters also include capacitors. In this case, minimization of the total reactive power of filter capacitors can be performed along with solving the optimal control problem.

The filter optimization problem includes constraints regarding EMC and power quality in WPS nodes. Power quality in WPS is presented by electric power quality indices, *THD* and *DPF*. The constraints relate the filter component values to the electric power quality indices. Constraints can be specified e.g. for the capacitors' peak voltage and the WPS frequency response. The latter addresses the EMC requirements.

The spectral technique for power quality and EMC design includes the following steps (see Fig. 2).

Step 1. *Specifying WPS structure and parameters.* WPS elements are defined by component values (resistance, inductance and capacitance), electrical characteristics (*e.g.* SG total power), and control parameters (*e.g.* commutation delay of an AC/DC converter).

Step 2. *Specifying desired power quality.* Desired power quality in WPS is presented by THD_D and DPF_D, specified according to power quality regulations. They are brought to a matrix $EPQ_{desired}$. Each row in *EPQ*-matrix corresponds to a node in WPS, and each column corresponds to a power quality index.

Step 3. *Specifying desired EMC.* In order to identify EMC problem in WPS, a designer uses regulations for conducted emissions, related to the equipment's power supplies connected to WPS.

Step 4. *Calculation of voltage and current spectra.* The calculation procedure utilizes a complete mathematical model of WPS to reflect essential non-linear processes in elements of WPS. A set of ordinary differential equations with discontinuous right-hand sides is numerically solved in time domain. The FFT technique is then used for calculating current and voltage spectra in WPS.

Step 5. *Forming an updated EPQ-matrix*. Calculated voltage and current spectra are used for forming an updated *EPQ*-matrix ($EPQ_{updated}$). *THD* and *DPF* are calculated according to the following well-known equations in the node of WPS where power quality is monitored:

$$THD = (\sum_{n=2}^{N} U_n^2)^{1/2} \; / \; U_1 \,, \tag{1}$$

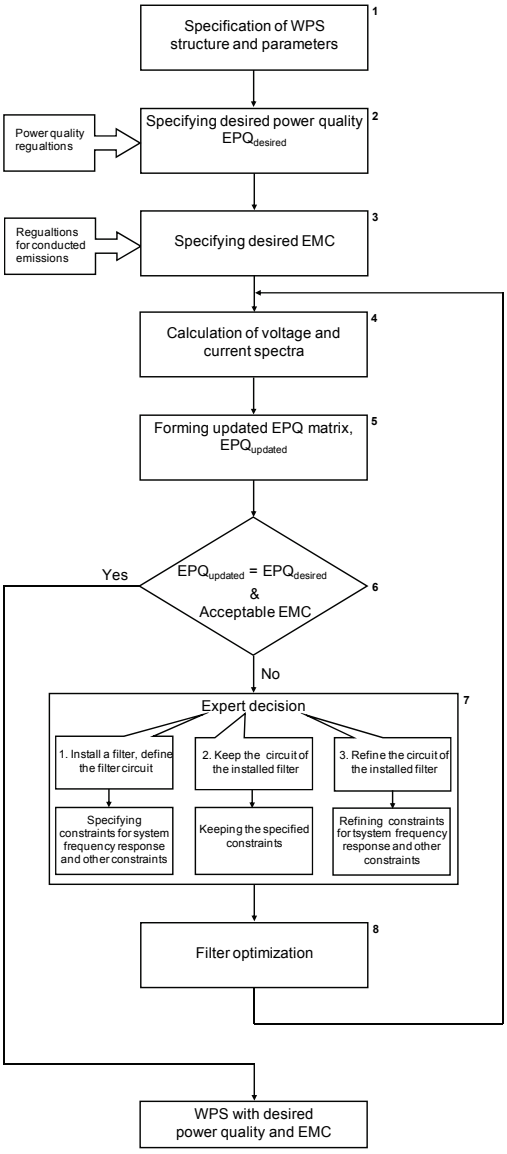

Fig. 2. Block diagram of the simulation-based spectral technique

$$DPF = (\sum_{n=1}^{N} U_n \cdot I_n \cdot \cos\varphi_n) / (\sum_{n=1}^{N} U_n^2 \sum_{n=1}^{N} I_n^2)^{1/2} \quad (2)$$

Step 6. *Comparing $EPQ_{updated}$ with $EPQ_{desired}$ and identifying EMC/power quality problem.* The desired *EPQ*-matrix is subtracted from the updated *EPQ*-matrix. If the matrix difference contains elements with the absolute values smaller than tolerance values

specified for each power quality index, then the power quality problem has been solved. Additionally, voltage and/or current spectra at the power supplies' output have to be compared with EMC regulations for conducted emissions. If a power quality and/or an EMC problem are identified, an expert decision has to be taken. Otherwise, the design process is finished.

Step 7. *Expert decision.* At the first pass of the algorithm the expert decision is installing a filter in the node of WPS with a poor power quality or EMC The choice of filter circuit and the filtered frequencies depends on the *EPQ*-matrices, the tolerance values, and the rms-values of current harmonics. Constraints for the WPS frequency response are specified by the designer. Some other constraints can be included, e.g. for the filter capacitors' peak voltage. These constraints will be used in the filter optimization procedure along with the power quality requirements defined in step 2. At the next passes of the algorithm two types of expert decision are possible. One of them is direct passing to step 8 with current and voltage spectra calculated in step 4 as the new input data for filter optimisation. Since the filter circuit has not been refined, the constraints are unchanged. The other expert decision is refinement of the filter circuit. In case of designing a passive filter, a resonant section can be added to the filter circuit. For an active or a hybrid filter, the refinement of the filter circuit would consist *e.g.* in adding passive components. Refinement of the filter circuit might lead to changing the constraints.

Step 8. *Filter optimisation.* The non-linear model is replaced by an algebraic model of WPS including the filter. Filter component values are determined by solving a non-linear programming problem, given the constraints for power quality indices (defined by $EPQ_{desired}$), for EMI (the WPS frequency response), and other constraints. The total reactive power of filter capacitors can be used as the minimization criterion-minimized.

Checking the filter performance is implemented by passing to step 4, where current and voltage spectra are calculated taking into account the power filter designed in step 8. Passing to step 4 can be explained by loss of some properties of WPS due to the simplified algebraic model neglecting non-linear properties of the filter in step 8. $EPQ_{updated}$ is then compared to $EPQ_{desired}$, and emission levels are compared to EMC regulations (step 6). A new expert decision is made (step 7), *etc*.

An example of application of the presented spectral technique, including a harmonic filter optimization is provided in (Belov et al., 2006). The optimization method was chosen from (Himmelblau, 1972).

3. Multi-phase electric power supply system modeling methodology

3.1 Multy-phase system elements and modeling requirements

Multi-phase electric power supply systems with the number of phases $p > 3$ have a number of advantages as compared to conventional three-phase systems. They include lower installed power of ac-machines at fixed dimensions, more compact power transmission line at equal carrying power, lower current loading per phase to result in lower-power semiconductor devices and more compact control equipment, wider range of speed control, and lower level of noise and vibration for electrical machines. Analysis and design methods for multi-phase electric power supply systems have been addressed by a number of authors, e.g. in (Binsaroor et al., 1988), (Toliyat et al., 2000). However, they are still not well

developed for independent power supply systems, where generated power and the consumed power are comparable. The tendency to consider multi-phase systems in the variant design (Brown et al., 1989) should be addressed in the modelling software enabling a common CAD environment for electric power supply systems, consisting of elements with different number of phases in feeding lines.

A general multi-phase electric power supply system includes a *p*-phase synchronous generator SG (*p* is a prime integer), power transmission line, an AC/DC/AC power converter and an ac-load. Additional multi-phase filters can be included in the power system.

Reducibility to a canonical form is the main requirement the mathematical models of power system's elements have to satisfy. It is related to the properties of a CAD tool designed for integrating element models to the complete mathematical model of the electric power supply system. The canonical form for mathematical models of the *p*-phase system elements is given by equation (3):

$$\frac{d}{dt} i_{dq0} = B u_{dq0} + D \tag{3}$$

where i_{dq0} is the vector of phase currents of a multi-phase element in *dq0* rotating coordinate system obtained by transformation from the multi-phase stationary coordinate system; B is the matrix containing the parameters of the modelled element (SG, AC/DC/AC converter, ac-load, and filters); u_{dq0} is the vector of phase voltages in the node where the multi-phase element is connected to the power transmission line, D is the vector dependent of i_{dq0}. Vector D is recalculated in each step of integration of equation (3).

Integrating of the models of the system elements into the complete mathematical model of the multi-phase electric power supply system is performed by means of equation (4) for multi-phase power transmission line (Belov, 1993):

$$U_{dq0} = -(K_1 + LK_2B_\Sigma)^{-1}(LK_2D_\Sigma + (LK_2^{'} + RK_2)I_{dq0\Sigma}), \tag{4}$$

where $K_2^{'} = dK_2 / dt$, $L = diag(L_j)$, $R = diag(R_j)$, $j = 1, 2, \ldots, N$, and N is the number of nodes in the power transmission line. Block-matrices K_1 and K_2 describe the structure of the power transmission line. Being multiplied by the vector of node voltages $U_{dq}0$, sub-diagonal block-matrix K_1 expresses the potential difference between the neighbouring nodes. The number of columns and the number of rows in this block-matrix are equal to the number of nodes in the power transmission line. An element of block-matrix K_1 is a non-zero matrix when an interconnecting line is connected to the corresponding nodes. Super-diagonal block-matrix K_2 is for reduction of the node currents contained in vector $I_{dq0\Sigma}$ to a base coordinate system. The base coordinate system can be a *dq0* system of any synchronous generator. This is the case when several generators are connected to the power transmission line. The rows and columns of matrix K_2 are constructed similarly to matrix K_1. The row corresponding to the interconnecting line where the selected generator is connected is filled with only non-zero matrices, since the current of this line is the sum of all node currents. A node current, in its turn, is the sum of currents through the system's elements, connected to a particular node of the power transmission line. In the other rows of block-matrix K_2, non-zero matrices are placed on the crossing with the columns corresponding to the nodes,

whose currents are summated in a particular interconnecting line. Block-matrices K_1, K_2 are built of matrices $\begin{bmatrix} \cos\delta_{ij} & \sin\delta_{ij} \\ -\sin\delta_{ij} & \cos\delta_{ij} \end{bmatrix}$ and $\begin{bmatrix} \cos\delta_{ij} & -\sin\delta_{ij} \\ \sin\delta_{ij} & \cos\delta_{ij} \end{bmatrix}$, where δ_{ij} is determined from equation (5):

$$(d\delta_{ij} / dt) = \omega_i - \omega_j , \tag{5}$$

where ω_i and ω_j are the angular speed values for rotating *dq0* coordinate systems in the neighboring nodes of the power transmission line.

3.2 Model of multi-phase synchronous generator

For mathematical modelling of power system elements with arbitrary number of electrical phases, it is necessary to have a general operator C_P. It can be obtained in the process of construction of the mathematical model for the *p*-phase synchronous generator (*p* is a prime integer, which can be represented as $p = 2k+1$, $k = 1, 2, 3, 5, \ldots$) (Belov et al., 2004). Let us consider SG with *p*+3 magnetically coupled circuits: *p* phase windings which are stationary and three rotor circuits which are rotating: one drive circuit and two damping circuits. The phase windings are supposed to be connected to the power transmission line. The drive circuit is connected to an *emf* source. The equilibrium equations for voltages in the rotor and stator circuits can then be written in a matrix form as follows:

$$\frac{d\Psi}{dt} + Ri + e = 0 , \tag{6}$$

where $R = diag(r, r, ..., r, r_D, r_Q, r_r)$ is a diagonal matrix, r is the resistance of each phase winding, r_D and r_Q are the resistances of the damping circuits, r_r is the resistance of the drive circuit; $i = \left[i_1, i_2, ..., i_p, i_D, i_Q, i_r\right]^T$ is the unknown vector of currents in the SG circuits, i_j, $j = 1, 2, ..., p$, are the phase currents, i_D and i_Q are the currents in the dumping circuits, i_r is the current in the drive circuit; $e = \left[e_1, e_2, ..., e_p, 0, 0, -e_r\right]^T$ is the known voltage vector, e_1, e_2, ..., e_{2k}, e_p are the voltages in the nodes of connection of the phase windings to the power transmission line, e_r is the voltage of the drive circuit; Ψ is the magnetic linkage vector for SG circuits, such that $\Psi = Li$, and L is the square matrix of the coefficients of self-induction and mutual induction for SG circuits, which is a symmetric matrix for physical reasons. The elements of matrix L are π - or 2π -periodic functions of angle γ. Angle γ is the angle between the magnetic axis of the first phase winding of SG and the longitudinal rotor axis at counter clockwise rotation.

Equations (6) have periodic coefficients. With the help of the 2π -periodic transformation matrix $C_P = C_P(\gamma)$, equation system (6) can be rewritten in a rotating *dq0* coordinate system, which corresponds well to a symmetric nature of the synchronous generator SG with poles. Matrix C_P has a dimension of $p \times p$ and is given by equation (7):

$$C_{P\,ij} = \begin{cases} 1/p, & \text{if } i = 1; \\ (2/p)\cos(\gamma - (j-1)n\rho), & \text{if } i = 2n-1, n \geq 2; \\ -(2/p)\sin(\gamma - (j-1)n\rho), & \text{if } i = 2n, n \geq 1. \end{cases} \tag{7}$$

In equation (7), $n \in \mathrm{N}$, $\rho = 2\pi / p$ is the angle between magnetic axes of adjacent phase windings. Here, $\det(C_P) = \pm\sqrt{\frac{2^{p-1}}{p^p}}$, i.e. determinant of matrix C_P is not equal to zero at all γ. Matrix $C = diag(C_P, 1, 1, 1)$ with a dimension of $(p+3)\times(p+3)$ can be obtained by complementing matrix C_P by an identity matrix. Let us now pre-multiply equation system (6) by matrix C keeping the following designations: $i_{dq0} = Ci$, $e_{dq0} = Ce$, $i_{dq0} = \left[i_0, i_{1,d}, i_{1,q}, i_{2,d}, i_{2,q}, \ldots, i_{k,d}, i_{k,q}, i_D, i_Q, i_r\right]^T$, and $e_{dq0} = \left[e_0, e_{1,d}, e_{1,q}, e_{2,d}, e_{2,q}, \ldots, e_{k,d}, e_{k,q}, e_D, e_Q, e_r\right]^T$. Performing a number of trigonometric calculations results in equation system (8) below, where $\omega = \dot{\gamma} = d\gamma / dt$ is the rotor angular speed.

$$\begin{cases} (r + L_0 \frac{d}{dt}) i_0 = -e_0 \\ (r + L_d^{(1)} \frac{d}{dt}) i_{1,d} - \omega L_q^{(1)} i_{1,q} + m_{sr} \frac{d}{dt} i_r + m_{sD} \frac{d}{dt} i_D - \omega m_Q i_Q = -e_{1,d} \\ (r + L_q^{(1)} \frac{d}{dt}) i_{1,q} + \omega (L_d^{(1)} i_{1,d} + m_{sr} i_r + m_{sD} i_D) + m_Q \frac{d}{dt} i_Q = -e_{1,q} \\ (r + L_d^{(2)} \frac{d}{dt}) i_{2,d} - \omega L_q^{(2)} i_{2,q} = -e_{2,d} \\ (r + L_q^{(2)} \frac{d}{dt}) i_{2,q} + \omega L_d^{(2)} i_{2,d} = -e_{2,q} \\ \quad \ldots\ldots\ldots\ldots\ldots\ldots \\ \frac{p}{2} m_{sD} \frac{d}{dt} i_{1,d} + (r_D + L_D \frac{d}{dt}) i_D + m_{rD} \frac{d}{dt} i_r = 0 \\ \frac{p}{2} m_{sQ} \frac{d}{dt} i_{1,q} + (r_Q + L_Q \frac{d}{dt}) i_Q = 0 \\ \frac{p}{2} m_{sr} \frac{d}{dt} i_{1,d} + (r_r + L_r \frac{d}{dt}) i_r + m_{rD} \frac{d}{dt} i_D = e_r \end{cases} \quad (8)$$

Coefficients L_0, $L_d^{(s)}$, $L_q^{(s)}$, s = 1, 2, ..., k, are now independent of angle γ. The coefficients of mutual induction between the phase windings can be sub-divided into k different sets (upper index in parentheses) according to the angle between the magnetic axes of phase windings that can take k different values: ρ, 2ρ, ..., $k\rho$, $k = \left[\frac{p}{2}\right]$. E.g., the first set includes mutual inductances of the windings, which are adjacent to each another along the stator bore, i.e. the angle between their magnetic axes equates ρ radians.

Symbol m with a lower index is used in equation system (8) for designation of the other coefficients of mutual induction. Symbols *s, r, D, Q* represent stator windings, drive circuit and two damping circuits (corresponding to *d*-axis and *q*-axis in the *dq0* coordinate system), respectively.

Extraction from equations (8) of the vector of time derivatives of SG phase currents leads to the canonical form of the SG model, expressed by equation (3).

3.3 Model of multiphase AC-load

Let us now make use of the transformation matrix C_P for derivation of an ac-load model in the form of equation (3). Differential equation expressing for ac-load in phase coordinates is represented by equation (9):

$$u = Ri + L\frac{d}{dt}i \tag{9}$$

where $R = diag(r_1,...,r_p)$; $L = diag(l_1,...,l_p)$; $u = \left[u_1,...,u_p\right]^T$; $i = \left[i_1,...,i_p\right]^T$; r_j, l_j, u_j, i_j are the resistances, inductances, voltages and currents, respectively, for each phase of the ac-load, j = 1, ..., p, $p \geq 3$.

Pre-multiplying equation (9) by matrix C_P and assuming $C_P u = u_{dq0} = \left[u_0, u_{1,d}, u_{1,q},..., u_{k,d}, u_{k,q}\right]^T$ and $C_P i = i_{dq0} = \left[i_0, i_{1,d}, i_{1,q},..., i_{k,d}, i_{k,q}\right]^T$ results in equation (10), written in a dq0 coordinate system:

$$u_{dq0} = Si_{dq0} + M\frac{d}{dt}i_{dq0}, \tag{10}$$

where $S = C_P R C_P^{-1} + C_P L\frac{d}{dt}C_P^{-1}$, $M = C_P L C_P^{-1}$.

Finally, pre-multiplying equation (10) by matrix M^{-1} would give the mathematical model of the ac-load in the canonical form (see equation (3)), where $B = M^{-1}$, and $D = -M^{-1}Si_{dq0}$.

4. Complete mathematical model of wind power system with integrated active filter

4.1 Statement of problem

In this section, a complete mathematical model will be built for the WPS presented in Fig. 1. The canonical form of mathematical models of the power system elements is given by (3). Integration of the models of the system elements into the complete mathematical model of the multi-phase electric power supply system is performed by means of equation (4).

Based on both the first Kirchoff's law and equation (3) for the *n*-th node of the power transmission line, equation (11) can be written under assumption that there are *k* elements connected to this node:

$$\frac{d}{dt}I_{dq0_{\Sigma n}} = \left(\sum_{i=1}^{k} B_{in}\right)U_{dq0_n} + \sum_{i=1}^{k} D_{in} = B_{\Sigma n}U_{dq0_n} + D_{\Sigma n} \tag{11}$$

It follows from (11) that in (4), B_Σ is the block-matrix constructed from matrices $B_{\Sigma n}$, vector D_Σ is constructed from sub-vectors $D_{\Sigma n}$, and vector I_{dq0_Σ} is constructed from sub-vectors $I_{dq0_{\Sigma n}}$.

The problem to be solved is thus formulated as developing of mathematical models of the AC/DC/AC converter and SMPS in the form (3), with the following integration of the developed element models into the mathematical model of the WPS by using equation (4).

Note that the active filter 1 model in the form (3) is derived in (Belov et al., 2005). It is also proposed to replace harmonic filter 2 with an active filter integrated into the control system of the load side voltage inverter (hereafter referred to as the voltage inverter), which compensates low frequency voltage and current harmonics. Moreover, the proposed active filter enables filtering of high frequency conducted emissions from a single-phase non-linear load, in the studied case represented by a switch mode power supply (SMPS) of electronic equipment. The active filter integrated in the AC/DC/AC converter is based on the PWM technique.

4.2 Multi-phase B-element concept

It was shown in (Belov, 1998), (Belov et al., 2005), (Belov, 1993) that most of electric power conversion circuits can be represented by a combination of bridge elements or B-elements, independently of the number of electrical phases. Thus, an m-phase B-element can be defined both by an equivalent graph and by a state scale for the graph edges. The principle of how to construct the equivalent graph of a B-element is shown in Fig. 3.

In general, the equivalent circuit of B-element contains $2m$+2 switching elements (see Fig. 3). Among them, $2m$ switching elements are the operating elements. Besides, there are a shunt switching element ($2m$+1) and a switching element referenced as $2m$+2, which is connected in series with the resistive-inductive load (R_{load}, L_{load}). Designations R^i and L^i stand for resistance and inductance of the feeding transformer winding, respectively; R_{S_1}, R_{S_2}, …, $R_{S_{2m+2}}$ and L_{S_1}, L_{S_2}, …, $L_{S_{2m+2}}$ are the resistances and inductances of typical branches of the B-element (see Fig. 3). The bridge element is fed from the p-phase ac-power transmission line (p is a prime integer). Here, i = 1, 2, …, m are the nodes where the bridge element is connected to the power transmission line. It is clear, that $m \le p$, and when a single-phase B-element is connected to the phase voltage, it is assumed that m = 2.

The equivalent directed graph has three vertices O, D, and E connected with $2m$+2 edges. The graph is obtained by removing some of the nodes from the equivalent circuit in order to combine the B-element typical branches (including the switching elements S_1, …, S_{2m}) with the branches representing the feeding transformer windings.

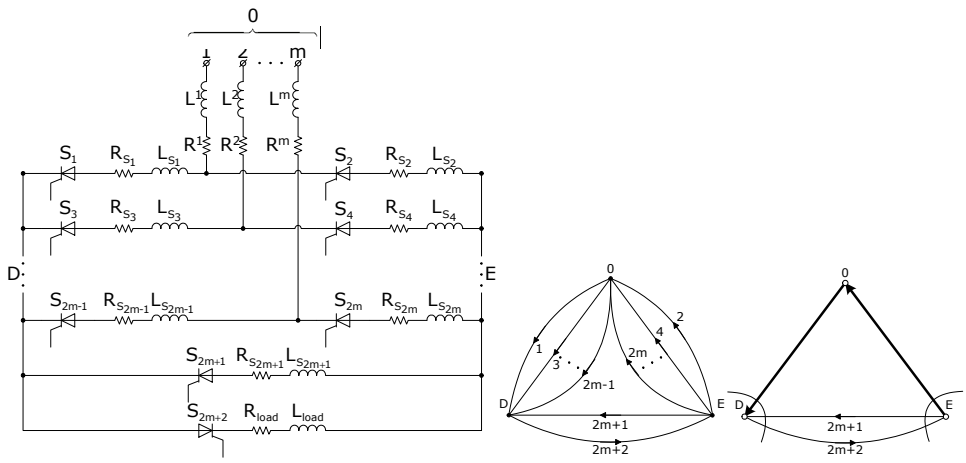

Fig. 3. Equivalent circuit of m-phase B-element and its equivalent graph.

The state scale Λ_S is a row-matrix consisting of 2*m*+2 elements. Each element characterizes the state of a single switching element, and equal to either 1 (closed) or 0 (open). The state scale should be related to equivalent graph's edges, with 1 indicating a conducting edge and 0 indicating a non-conducting edge.
The B-element concept is a convenient tool for mathematical modelling of multi-phase semiconductor rectifiers, inverters, active filters and complex combinations thereof. Mathematical models of single- and three-phase devices are obtained as a particular case of multi-phase B-element concept.

4.3 Integrated active filter

A functional block diagram of the control system of the voltage inverter is shown in Fig. 4.
It includes two control channels: channel 1 (low frequency) and channel 2 (high frequency). Channel 1 affects switches $S_3^{(1)}$ and $S_4^{(1)}$, and channel 2 affects switches $S_1^{(1)}$ and $S_2^{(1)}$. Such a channel division is implemented in order to simplify the control system and reduce the total cost of the switching elements (transistors). Superscript "(1)" distinguishes the switches in the AC/DC/AC converter from those in the voltage inverter.
Channel 1 forms rectangular pulse train with a duration of 180 electrical degrees, and with the fundamental frequency 60 Hz set by sinusoidal voltage U_{sin}, according to the following algorithm. Signal U_{sin} is supplied to the input of comparator K_1. In case of positive input signal, a high-level control signal is formed at the output of K_1, which is in its turn supplied both to repeater D_3 and to logic inverter D_4 (element NOT). The signal from D_3 is supplied to switch $S_3^{(1)}$ to close it. Logic inverter D_4 inverts the signal from the K_1 output and supplies it to switch $S_4^{(1)}$, thereby to open it. In case of negative input signal, a low-level control signal is formed on the output of comparator K_1, which, in its turn, passing through D_3 and D_4 opens switch $S_3^{(1)}$ and closes switch $S_4^{(1)}$.

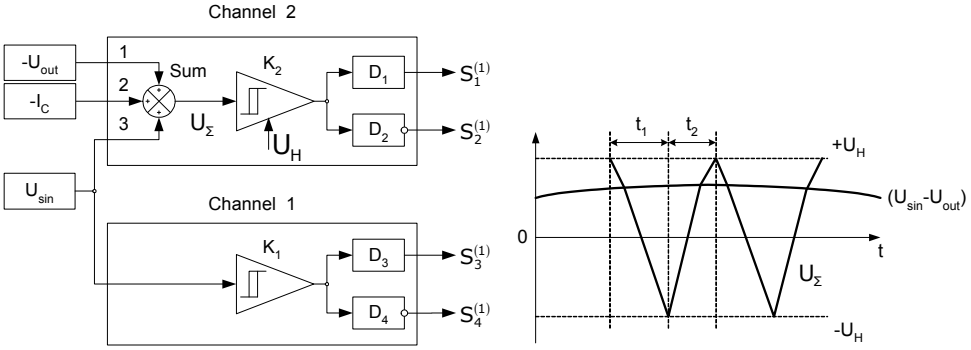

Fig. 4. Functional block diagram of the voltage inverter control system and formation of the high frequency pulse train in channel 2

Channel 2 forms high frequency control pulses with parameters depending on the inverter output voltage deviation from the reference voltage, (U_{sin} - U_{out}). The instant output voltage deviation corresponds to the total conducted interference in the node of the load (SMPS) connection. Channel 2 is used for controlling the level of harmonic voltages on the inverter output. The high frequency control channel, switches $S_1^{(1)}$ and $S_2^{(1)}$ along with the output Γ-filter of the voltage inverter are the elements of the integrated active filter.

The active filter operates against conducted emissions in the following manner. Input 1 of summator Sum is supplied with the signal U_{out} from the voltage sensor placed on the inverter output. Input 2 is supplied with current I_C from the current sensor, corresponding to the current through the capacitor of the output Γ-filter (see Fig.1 and Fig. 4). Input 3 of summator Sum is supplied with voltage U_{sin}. The summed signal is supplied to comparator K_2. If the input signal exceeds the threshold level $+U_H$, a high-level control signal is formed on the K_2 output, which is then supplied both to repeater D_1 and to logic inverter D_2. The signal of D_1 is supplied to switch $S_1^{(1)}$, to close it. Logic inverter D_2 inverts the signal and supplies it to switch $S_2^{(1)}$ thereby opening this switch. If the input signal is below the threshold level $-U_H$, a low-level control signal is formed in the K_2 output, which by means of blocks D_1 and D_2, opens switch $S_1^{(1)}$ and closes switch $S_2^{(1)}$.

The process of forming the high frequency pulse train in channel 2 is shown in Fig. 4. Let us consider this process during the time interval where the positive half-wave of the inverter output voltage is formed. Here switch $S_3^{(1)}$ is closed and switch $S_4^{(1)}$ is open, and the high-level control signal is formed in the K_2 output (switch $S_1^{(1)}$ is closed, and switch $S_2^{(1)}$ is open). This state of the switches enables discharging of the capacitor of the output Γ-filter through $S_1^{(1)}$ and $S_3^{(1)}$, to result in lowering the voltage on the load.

This shows us the role of the output Γ-filter as a part of the integrated active filter. The voltage signal corresponding to $-I_C$ is added to the difference (U_{sin} - U_{out}), and the summed signal U_Σ starts to decrease down to the level $-U_H$. When the summed signal in the K_2 input reaches level $-U_H$, a low-level control signal is formed in the K_2 output, so that switch $S_1^{(1)}$ is closed whereas switch $S_2^{(1)}$ is opened. At this moment of time current I_C changes the direction and the summed signal U_Σ in the K_2 input starts to increase up to level $+U_H$. When comparator K_2 changes its state, a high-level control signal is formed in its output, so that switch $S_1^{(1)}$ is opened and switch $S_2^{(1)}$ is closed.

Described above is the single operating cycle of channel 2, where t_1 and t_2 are the time intervals of $S_1^{(1)}$ and $S_2^{(1)}$ operation, respectively. On the time interval where the negative half-wave is formed, switch $S_4^{(1)}$ is closed and switch $S_3^{(1)}$ is opened, so that the whole picture of pulse train formation is just mirrored. The frequency of operating cycles depends on the output Γ-filter parameters and the level of U_H of comparator K_1.

4.4 Mathematical model of the AC/DC/AC converter

An equivalent circuit of the AC/DC/AC converter presented in Fig. 5 is built according to the multi-phase bridge-element concept. The studied AC/DC/AC converter is described by two bridge elements (*B*-elements) with typical branches composed from a switching element, a resistor and an inductor. The equivalent circuit of the voltage inverter is represented by *B*-element B_1, whereas the equivalent circuit of the rectifier is represented by *B*-element B_2. Superscript "1" is assigned to the elements of the single-phase voltage inverter, and superscript "2" is assigned to the elements of the three-phase rectifier.

The following designations are used in Fig. 5: 1, 0 are the points of connection of the AC/DC/AC converter to the single-phase power line; *a*, *b*, *c* are the points of connection of the AC/DC/AC converter to the power generator; $R_1^{(1)}$, $R_0^{(1)}$ are the output resistances of the inverter; $L_1^{(1)}$, $L_0^{(1)}$ are the output inductances of the inverter; $S_i^{(1)}$, $R_{S_i}^{(1)}$, $L_{S_i}^{(1)}$ are the switching element, resistance and inductance, respectively, placed in the *i*-th (i = 1, 2, 3, 4)

branch of the inverter bridge; $C_5^{(1)}$ is the capacitor to accumulate electric power, performing as battery (DC capacitor in Fig. 1); $S_5^{(1)}$, $R_{S_5}^{(1)}$, $L_{S_5}^{(1)}$ are the elements found in the circuit of battery $C_5^{(1)}$; $S_1^{(X)}$, $R_{S_1}^{(X)}$, $L_{S_1}^{(X)}$ are the elements corresponding to the output choke of the rectifier; $S_i^{(2)}$, $R_{S_i}^{(2)}$, $L_{S_i}^{(2)}$ are the elements placed in the *i*-th (*i* = 1, 2,…, 6) branch of the three-phase rectifier bridge; $R_1^{(2)}$, $R_2^{(2)}$, $R_3^{(2)}$ are the input resistances of the rectifier; $L_1^{(2)}$, $L_2^{(2)}$, $L_3^{(2)}$ are the input inductances of the rectifier; $S_7^{(1)}$, $R_{S_7}^{(1)}$, $L_{S_7}^{(1)}$ are the elements found in the circuit of the voltage sensor in the rectifier output.

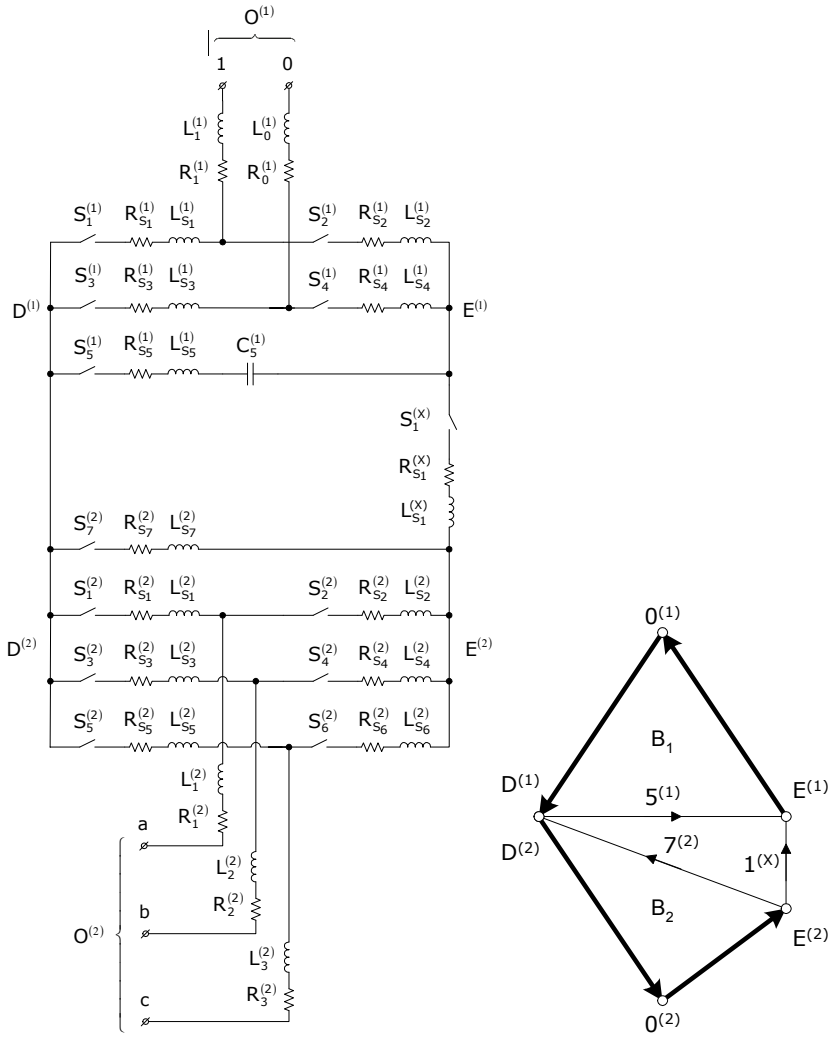

Fig. 5. Equivalent circuit of the AC/DC/AC converter, and its equivalent graph.

In Fig. 5 a graph is presented, that corresponds to the equivalent circuit of the AC/DC/AC converter. The main principles of forming the graph are reported in (Belov et al., 2005). Thickened arcs in the graph include the elements connected in series, in the equivalent circuit. For example, arc $O^{(1)}D^{(1)}$ consists of two adjacent edges. The first edge includes elements $L_1^{(1)}$, $R_1^{(1)}$, $L_{S_1}^{(1)}$, $R_{S_1}^{(1)}$, $S_1^{(1)}$ connected in series, and the second edge includes elements $L_0^{(1)}$, $R_0^{(1)}$, $L_{S_3}^{(1)}$, $R_{S_3}^{(1)}$, $S_3^{(1)}$.

Graphs of *B*-elements B_1 and B_2 are combined in the graph of the AC/DC/AC converter by means of chord $1^{(X)}$. Below is the equation for voltages related to the graph edges:

$$V = U_S + ZI + NU_{abc} + MU_C \tag{12}$$

where $V = \left[\left(V^{(1)}\right)^T, \left(V^{(2)}\right)^T, \left(V^{(X)}\right)^T\right]^T$, $I = \left[\left(I^{(1)}\right)^T, \left(I^{(2)}\right)^T, \left(I^{(X)}\right)^T\right]^T$. Here $V^{(1)}$, $V^{(2)}$ are the vectors of voltages, $I^{(1)}$, $I^{(2)}$ are the vectors of currents related to the graph edges corresponding to B_1 and B_2; $V^{(X)}$, $I^{(X)}$ are the voltage and current, respectively, related to edge $1^{(X)}$. Besides, $U_S = \left[\left(U_S^{(1)}\right)^T, \left(U_S^{(2)}\right)^T, \left(U_S^{(X)}\right)^T\right]^T$, and $U_S^{(1)}$, $U_S^{(2)}$ are the vectors of voltages on the switching elements of B_1 and B_2 respectively; $U_S^{(X)}$ is the voltage on the switching element of chord $1^{(X)}$ (note that $U_S^{(X)} = 0$, since this edge is always conducting); $U_{abc} = \left[\left(U_{abc}^{(1)}\right)^T, \left(U_{abc}^{(2)}\right)^T\right]^T$, $U_{abc}^{(1)}$, $U_{abc}^{(2)}$ are the vectors of phase voltages in the nodes of connection of the first and of the second *B*-elements to the single-phase power line and to the three-phase power generator, respectively (note that both the second and the third elements of vector $U_{abc}^{(1)}$ are equal to zero); $Z = j\omega L + R$, and R, L are the matrices containing resistances and inductances, respectively, related to the graph edges; $R = diag(R^{(1)}, R^{(2)}, R^{(X)})$, and $R^{(1)}$, $R^{(2)}$ are the matrices containing resistances related to the graph edges of the respective *B*–elements, and $R^{(X)} = R_{S_1}^{(X)}$ is the resistance of edge $1^{(X)}$; $L = diag(L^{(1)}, L^{(2)}, L^{(X)})$, and $L^{(1)}$, $L^{(2)}$ are the matrices containing inductances related to the graph edges of the respective *B*–elements, and $L^{(X)} = L_{S_1}^{(X)}$ is the inductance of edge $1^{(X)}$; U_C is the voltage on $C_5^{(1)}$; M is the vector which forms the 5^{th} column in the (13×13) unity matrix; $N = \begin{bmatrix} diag(N^{(1)}, N^{(2)}) \\ N^{(X)} \end{bmatrix}$, $N^{(X)}$ is the (1×6) null row matrix. Matrices $R^{(1)}$ and $R^{(2)}$ have the following structure:

$$R^{(1)} = \begin{bmatrix} R_{S_1}^{(1)} + R_1^{(1)} & -R_1^{(1)} & 0 & 0 & 0 \\ -R_1^{(1)} & R_{S_1}^{(1)} + R_1^{(1)} & 0 & 0 & 0 \\ 0 & 0 & R_{S_3}^{(1)} + R_2^{(1)} & -R_2^{(1)} & 0 \\ 0 & 0 & -R_2^{(1)} & R_{S_4}^{(1)} + R_2^{(1)} & 0 \\ 0 & 0 & 0 & 0 & R_{S_5}^{(1)} \end{bmatrix},$$

$$R^{(2)} = \begin{bmatrix} R_{S_1}^{(2)} + R_1^{(2)} & -R_1^{(2)} & 0 & 0 & 0 & 0 & 0 \\ -R_1^{(2)} & R_{S_2}^{(2)} + R_1^{(2)} & 0 & 0 & 0 & 0 & 0 \\ 0 & 0 & R_{S_3}^{(2)} + R_2^{(2)} & -R_2^{(2)} & 0 & 0 & 0 \\ 0 & 0 & -R_2^{(2)} & R_{S_4}^{(2)} + R_2^{(2)} & 0 & 0 & 0 \\ 0 & 0 & 0 & 0 & R_{S_5}^{(2)} + R_3^{(2)} & -R_3^{(2)} & 0 \\ 0 & 0 & 0 & 0 & -R_3^{(2)} & R_{S_6}^{(2)} + R_3^{(2)} & 0 \\ 0 & 0 & 0 & 0 & 0 & 0 & R_{S_7}^{(2)} \end{bmatrix}.$$

Matrices $L^{(1)}$ and $L^{(2)}$ have a structure similar to matrices $R^{(1)}$ and $R^{(2)}$. Matrices $N^{(1)}$ and $N^{(2)}$ are the following:

$$N^{(1)} = \begin{bmatrix} 1/2 & 0 & 0 \\ -1/2 & 0 & 0 \\ -1/2 & 0 & 0 \\ 1/2 & 0 & 0 \\ 0 & 0 & 0 \end{bmatrix}, \; N^{(2)} = \begin{bmatrix} -1 & 0 & 0 \\ 1 & 0 & 0 \\ 0 & -1 & 0 \\ 0 & 1 & 0 \\ 0 & 0 & -1 \\ 0 & 0 & 1 \\ 0 & 0 & 0 \end{bmatrix}.$$

In order to determine the currents related to the conducting edges of the graph, and the voltages of the switching elements on the non-conducting graph edges, matrix operator C is constructed as follows:

$$C = \left[\begin{array}{c|c|c} C_B^{(1)} & 0 & 0 \\ \hline 0 & C_B^{(2)} & 0 \\ \hline C_X^{(1)} & C_X^{(2)} & 1 \end{array}\right],$$

where $C_B^{(1)}$, $C_B^{(2)}$ are the circuit matrices for independent directed cycles, formed by the chords of corresponding B-elements, $\left[C_X^{(1)}, C_X^{(2)}, 1\right]$ is the row-matrix for the independent directed cycle corresponding to chord $1^{(X)}$. All non-zero block-matrices forming matrix C are built on the basis of state scales $\Lambda_D^{(1)}$, $\Lambda_E^{(1)}$, $\Lambda_T^{(1)}$, $\Lambda_D^{(2)}$, $\Lambda_E^{(2)}$, $\Lambda_T^{(2)}$ corresponding to the tree edges of the respective B-elements. Particularly, $C_X^{(1)} = \Lambda_T^{(1)}$ and $C_X^{(2)} = \Lambda_T^{(2)}$. The tree edges are collected one by one from adjacent edges that form the thickened arcs of B-elements.

Let us consider the formation of state scales on the example of B-element B_1. A state scale is a row-matrix, with the number of elements equal to the number of edges in a B-element. First, the main state scale $\Lambda_S^{(1)}$ is formed corresponding to the states of switching elements of all B-element edges. After that, the state scales $\Lambda_D^{(1)}$ and $\Lambda_E^{(1)}$ are formed for the tree edges, which are incident to the fundamental cut-sets $D^{(1)}$ and $E^{(1)}$, respectively, see Fig. 5. State scale $\Lambda_D^{(1)}$ is constructed from state scale $\Lambda_S^{(1)}$ by placing in $\Lambda_D^{(1)}$ the first odd (by counting) non-zero element of $\Lambda_S^{(1)}$, and by assigning zero values to the rest elements.

Similarly, row-matrix $\Lambda_E^{(1)}$ is constructed from $\Lambda_S^{(1)}$, by leaving unchanged the first even (by counting) non-zero element of $\Lambda_S^{(1)}$, and by letting the other elements be zero-valued. Thus, the state scale of the tree becomes the following: $\Lambda_T^{(1)} = \Lambda_D^{(1)} + \Lambda_E^{(1)}$. For example, let us assume the edges 1, 4 and 5 to be conducting. In this case, $\Lambda_S^{(1)} = [1 \;\; 0 \;\; 0 \;\; 1 \;\; 1]$, $\Lambda_D^{(1)} = [1 \;\; 0 \;\; 0 \;\; 0 \;\; 0]$, $\Lambda_E^{(1)} = [0 \;\; 0 \;\; 0 \;\; 1 \;\; 0]$, $\Lambda_T^{(1)} = [1 \;\; 0 \;\; 0 \;\; 1 \;\; 0]$.

In order to construct block $C_B^{(1)}$ in block-matrix *C*, corresponding to *B*-element B_1, it is necessary to perform the following operations. State scale $\Lambda_D^{(1)}$ is subtracted from the odd rows (except the last one) of the unity matrix of the appropriate size, whereas state scale $\Lambda_E^{(1)}$ is subtracted from the even rows of the unity matrix. State scale $\Lambda_T^{(1)}$ should then be added to the last row of the obtained matrix. As result,

$$C_B^{(1)} = \begin{bmatrix} 0 & 0 & 0 & 0 & 0 \\ 0 & 1 & 0 & -1 & 0 \\ -1 & 0 & 1 & 0 & 0 \\ 0 & 0 & 0 & 0 & 0 \\ 1 & 0 & 0 & 1 & 1 \end{bmatrix}.$$

By rearranging the rows matrix *C* can be presented by two blocks, i.e. both by matrix C_L (for independent directed cycles, containing only conducting edges of the graph) and by matrix C_0 (for independent directed cycles, containing at least one non-conducting edge). Matrices C_L and C_0 contain the rows of matrix *C* with the numbers corresponding to the numbers of the elements valued to 1 in state scales Λ_L and Λ_O, respectively. State scales $\Lambda_L^{(1)}$ and $\Lambda_L^{(2)}$ corresponding to the closed circuits in the graphs of B_1 and B_2 are formed according to the following algorithms: $\Lambda_L^{(1)} = \Lambda_S^{(1)} - \Lambda_T^{(1)}$ and $\Lambda_L^{(2)} = \Lambda_S^{(2)} - \Lambda_T^{(2)}$. State scale Λ_L, corresponding to the closed circuits in the graph of the AC/DC/AC converter is formed as $\Lambda_L = [\Lambda_L^{(1)}, \Lambda_L^{(2)}, \Lambda_L^{(X)}]$, where $\Lambda_L^{(1)}$ and $\Lambda_L^{(2)}$ are state scales of *B*-elements B_1 and B_2, respectively, and $\Lambda_L^{(X)}$ is the state scale of the graph edge $1^{(X)}$; here $\Lambda_L^{(X)} = 1$, since this edge is always conducting. State scale Λ_O corresponding to the open circuits in the graph of the AC/DC/AC converter is formed according to logic expression, $\Lambda_{Oi} = \begin{cases} 1, & if \;\; \Lambda_{Li} = 0 \\ 0, & if \;\; \Lambda_{Li} = 1 \end{cases}$, where *i* is the number of a state scale element, $i = 1, 2, ..., 13$.

According to the second Kirchoff's law,

$$\begin{bmatrix} C_L \\ C_O \end{bmatrix} V = 0 \tag{13}$$

The currents related to the edges of the graph of the AC/DC/AC converter are given by (14):

$$I = C^T I_C = [C_L^T, C_O^T] \cdot \begin{bmatrix} I_L \\ I_O \end{bmatrix} = C_L^T I_L \tag{14}$$

where I_C is the vector of currents related to all independent directed cycles in the graph, I_L and I_O are the vectors of currents related to closed and open circuits in the graph, respectively. By definition, elements of vector I_O are always set to zero. Substitution of (12) and (14) into (13) leads to (15):

$$\begin{bmatrix} C_L \\ C_O \end{bmatrix} U_S + \begin{bmatrix} C_L \\ C_O \end{bmatrix} Z C_L^T I_L + \begin{bmatrix} C_L \\ C_O \end{bmatrix} N U_{abc} + \begin{bmatrix} C_L \\ C_O \end{bmatrix} M U_C = 0 \tag{15}$$

Let us now rewrite (15) in time domain, taking into account $Z = Lp + R$ and $C_L U_C = 0$, with p as the differentiation operator:

$$L_L \frac{d}{dt} I_L + R_L I_L + N_L U_{abc} + M_L U_C = 0 \tag{16}$$

$$U_O + L_O \frac{d}{dt} I_L + R_O I_L + N_O U_{abc} + M_O U_C = 0 \tag{17}$$

where $U_O = C_O U_S$, $L_L = C_L L C_L^T$, $R_L = C_L R C_L^T$, $N_L = C_L N$, $M_L = C_L M$, $L_O = C_O L C_L^T$, $R_O = C_O R C_L^T$, $N_O = C_O N$, $M_O = C_O M$. Equation (16) can be modified into (18), which is being subsequently substituted into (17) results in equation (19) for currents $I_L(t)$ related to conducting edges and for voltages $U_O(t)$ across the non-conducting edges of the graph.

$$\frac{d}{dt} I_L = -L_L^{-1} \left(R_L I_L + N_L U_{abc} + M_L U_C \right) \tag{18}$$

$$\begin{cases} \dfrac{d}{dt} I_L = Z_L I_L + L_{N_L} U_{abc} + L_{M_L} U_C \\ U_O = Z_O I_L + L_{N_O} U_{abc} + L_{M_O} U_C \end{cases} \tag{19}$$

where $Z_L = -L_L^{-1} R_L$, $Z_O = L_O L_L^{-1} R_L - R_O$, $L_{N_L} = -L_L^{-1} N_L$, and $L_{N_O} = L_O L_L^{-1} N_L - N_O$, $L_{M_L} = -L_L^{-1} M_L$, $L_{M_O} = L_O L_L^{-1} M_L - M_O$. System of equations (19) should be supplemented with differential equation (20) for voltage on capacitor $C_5^{(1)}$:

$$\frac{d}{dt} U_C = C_{C_L} I_L \tag{20}$$

where $C_{C_L} = \dfrac{1}{C_5^{(1)}} M^T C_L^T$. Combination of the first equation from system (19) with equation (20) leads to system of equations (21):

$$\begin{cases} \dfrac{d}{dt} \begin{pmatrix} I_L \\ \hline U_C \end{pmatrix} = \left(\begin{array}{c} L_{N_L} \\ \hline 0 \end{array} \right) U_{abc} + \left(\begin{array}{c|c} Z_L & L_{M_L} \\ \hline C_{C_L} & 0 \end{array} \right) \begin{pmatrix} I_L \\ \hline U_C \end{pmatrix} \\ U_O = Z_O I_L + L_{N_O} U_{abc} + L_{M_O} U_C \end{cases} \tag{21}$$

Multiplication of the first equation in system (21) by C_L^T and taking into account (14), result in (22):

$$\frac{d}{dt}I = C_L^T Z_L I_L + C_L^T L_{N_L} U_{abc} + C_L^T L_{M_L} U_C \tag{22}$$

In order to obtain the phase currents, equation (22) is left-sided multiplied by matrix $F = diag\left(F^{(1)}, F^{(2)}, 0\right)$, which consists of blocks, as follows:

$$F^{(1)} = \begin{bmatrix} 1 & -1 & 0 & 0 & 0 \\ 0 & 0 & 0 & 0 & 0 \\ 0 & 0 & 0 & 0 & 0 \end{bmatrix} \text{ and } F^{(2)} = \begin{bmatrix} 1 & -1 & 0 & 0 & 0 & 0 & 0 \\ 0 & 0 & 1 & -1 & 0 & 0 & 0 \\ 0 & 0 & 0 & 0 & 1 & -1 & 0 \end{bmatrix}.$$

Equation (23) is the result of the left-sided multiplication:

$$\frac{d}{dt}I_{abc} = F_{ZL} I_L + F_{LNL} U_{abc} + F_{LML} U_C \tag{23}$$

where $I_{abc} = \left[\left(I_{abc}^{(1)}\right)^T, \left(I_{abc}^{(2)}\right)^T\right]^T$, and $I_{abc}^{(1)}$, $I_{abc}^{(2)}$ are the vectors of phase currents in the nodes where B_2 and B_1 are connected to the corresponding power lines; $F_{ZL} = FC_L^T Z_L$, $F_{LNL} = FC_L^T L_{N_L}$ and $F_{LML} = FC_L^T L_{M_L}$.

Let us now make transformation of the three-phase coordinate system to the rotating *dq0* coordinate system. This is done by means of matrix operator C_{dq}:

$$\frac{d}{dt}\left(C_{dq}^{-1} I_{dq}\right) = F_{ZL} I_L + F_{LNL} C_{dq}^{-1} U_{dq} + F_{LML} U_C \tag{24}$$

where $C_{dq} = diag\left(C_p, C_p\right)$; C_p is the Park's transformation (Park, 1929); $I_{dq} = \left[\left(I_{dq}^{(1)}\right)^T, \left(I_{dq}^{(2)}\right)^T\right]^T$, and $U_{dq} = \left[\left(U_{dq}^{(1)}\right)^T, \left(U_{dq}^{(2)}\right)^T\right]^T$ are the vectors of images of phase currents and voltages in the *dq*0 coordinate system. A number of simple mathematical manipulations with (24) result in (25):

$$\frac{d}{dt}I_{dq} = C_{dq} F_{ZL} I_L + C_{dq} F_{LNL} C_P^{-1} U_{dq} + C_{dq} F_{LML} U_C - C_{dq} \frac{d}{dt}\left(C_{dq}^{-1}\right) I_{dq} \tag{25}$$

According to (20),

$$I_{dq} = C_{dq} I_{abc} = C_{dq} F I = C_{dq} F C_L^T I_L \tag{26}$$

Substitution of (26) into (25) leads to (27):

$$\frac{d}{dt}I_{dq} = C_{dq} F_{LNL} C_{dq}^{-1} U_{dq} + \left\{C_{dq} F_{ZL} - C_{dq} \frac{d}{dt}\left(C_{dq}^{-1}\right) C_{dq} F C_L^T\right\} I_L + C_{dq} F_{LML} U_C \tag{27}$$

At last, (27) can be represented in canonical form (3):

$$\frac{d}{dt} I_{dq} = BU_{dq} + D \tag{28}$$

where $B = C_{dq} F_{LNL} C_{dq}^{-1}$, $D = \left\{ C_{dq} F_{ZL} - C_{dq} \frac{d}{dt}\left(C_{dq}^{-1}\right) C_{dq} F C_L^T \right\} I_L + C_{dq} F_{LML} U_C$. Combination of (28) with equations (21) results in system of equations (29):

$$\begin{cases} \dfrac{d}{dt} I_{dq} = BU_{dq} + D \\ \dfrac{d}{dt}\begin{pmatrix} I_L \\ \hline U_C \end{pmatrix} = \begin{pmatrix} L_{N_L} \\ \hline 0 \end{pmatrix} C_{dq}^{-1} U_{dq} + \left(\begin{array}{c:c} Z_L & L_{M_L} \\ \hline C_{C_L} & 0 \end{array}\right) \begin{pmatrix} I_L \\ \hline U_C \end{pmatrix} \\ U_O = Z_O I_L + L_{N_O} C_{dq}^{-1} U_{dq} + L_{M_O} U_C \end{cases} \tag{29}$$

Equation system (29) is a system of differential and algebraic equations. It represents the mathematical model of the AC/DC/AC converter, connected to the three-phase power generator and to the single-phase power line.

Let us now consider interaction between the model of the AC/DC/AC converter (29) and the mathematical model of the control system of the voltage inverter, and thereby realization of high frequency channel control functions as the main element of the integrated active filter. According to the functional block diagram of the voltage inverter control system presented in Fig. 4, the main state scale for *B*-element B_1 is formed according to the following algorithm:

$$\begin{cases} \Lambda_{S_1}^{(1)} = \begin{cases} 1, & \begin{cases} if\ U_\Sigma > 0 \\ if\ -U_H \le U_\Sigma \le U_H, \quad if\ \left[\Lambda_{S_1}^{(1)}\right]_{prev} = 1 \end{cases} \\ 0, & \begin{cases} if\ U_\Sigma < 0 \\ if\ -U_H \le U_\Sigma \le U_H, \quad if\ \left[\Lambda_{S_1}^{(1)}\right]_{prev} = 0 \end{cases} \end{cases}, \quad \Lambda_{S_2}^{(1)} = \begin{cases} 1, & if\ \Lambda_{S_1}^{(1)} = 0 \\ 0, & if\ \Lambda_{S_1}^{(1)} = 1 \end{cases} \\ \Lambda_{S_3}^{(1)} = \begin{cases} 1, & if\ U_{\sin} > 0 \\ 0, & if\ U_{\sin} \le 0 \end{cases}, \quad \Lambda_{S_4}^{(1)} = \begin{cases} 1, & if\ \Lambda_{S_3}^{(1)} = 0 \\ 0, & if\ \Lambda_{S_3}^{(1)} = 1 \end{cases}, \quad \Lambda_{S_5}^{(1)} = 1 \end{cases} \tag{30}$$

where $\left[\Lambda_{S_1}^{(1)}\right]_{prev}$ is the previous state of $\Lambda_{S_1}^{(1)}$. Notice that $\Lambda_{S_5}^{(1)} = 1$ since there is element $C_5^{(1)}$ in the 5^{th} edge of the graph. The main state scale of B_2 is formed according to the following algorithm:

$$\Lambda_{S_i}^{(2)} = \begin{cases} 1, & if\ U_{S_i}^{(2)} > 0 \\ 0, & if\ I_{S_i}^{(2)} \le 0 \end{cases} \tag{31}$$

where *i* is the number of the state scale element, $i = 1, 2, ..., 6$.

4.5 Mathematical model of SMPS

An equivalent circuit of a switch mode power supply (Gottlieb, 1994) is shown in Fig. 6.

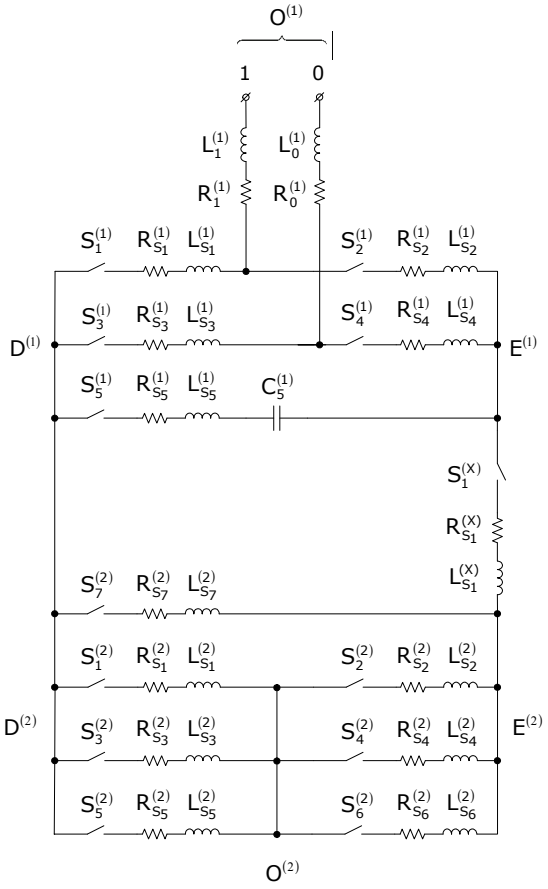

Fig. 6. Equivalent circuit of the SMPS.

The following designations are used in the figure: 0 and 1 are the nodes of connection of the SMPS to the single-phase power line; $R_1^{(1)}$ and $R_0^{(1)}$ are the input resistances; $L_1^{(1)}$ and $L_0^{(1)}$ are the input inductances; $S_i^{(1)}$, $R_{S_i}^{(1)}$, and $L_{S_i}^{(1)}$ are the switching element, resistance and inductance, respectively, in the *i*-th (i = 1, 2, 3, 4) section of the rectifier bridge; $C_5^{(1)}$ is the smoothing capacitor; $S_5^{(1)}$, $R_{S_5}^{(1)}$ and $L_{S_5}^{(1)}$ are the elements present in the smoothing capacitor circuit; $S_1^{(X)}$, $R_{S_1}^{(X)}$ and $L_{S_1}^{(X)}$ are the switching element, resistance and inductance, respectively, of the output choke of the rectifier; elements $S_1^{(2)}$, $R_{S_1}^{(2)}$ and $L_{S_1}^{(2)}$ represent a MOSFET; elements $S_2^{(2)}$, $R_{S_2}^{(2)}$ and $L_{S_2}^{(2)}$ model the load, referred to the primary winding of the SMPS transformer; elements $S_3^{(2)}$, $R_{S_3}^{(2)}$ and $L_{S_3}^{(2)}$ model the damping circuit of the MOSFET; $S_4^{(2)}$, $R_{S_4}^{(2)}$ and $L_{S_4}^{(2)}$ represent the load damper, including a diode; elements $S_i^{(2)}$, $R_{S_i}^{(2)}$ and $L_{S_i}^{(2)}$ are related to the voltage sensors (i = 5, 6, 7).

Let us apply the multi-phase bridge-element concept for building of the graph of the SMPS equivalent circuit. It can be shown that the resulting graph would be fully similar to the one presented in Fig. 5. Therefore, the mathematical model represented by (29) can be applied in SMPS analysis with the minor changes shown below. In case of SMPS, matrices $R^{(2)}$, $L^{(2)}$ corresponding to B_2, and matrix N are $R^{(2)} = diag\left(R_{S_1}^{(2)}, R_{S_2}^{(2)}, R_{S_3}^{(2)}, R_{S_4}^{(2)}, R_{S_5}^{(2)}, R_{S_6}^{(2)}, R_{S_7}^{(2)}\right)$, $L^{(2)} = diag\left(L_{S_1}^{(2)}, L_{S_2}^{(2)}, L_{S_3}^{(2)}, L_{S_4}^{(2)}, L_{S_5}^{(2)}, L_{S_6}^{(2)}, L_{S_7}^{(2)}\right)$, $N = \begin{bmatrix} N^{(1)} \\ 0 \end{bmatrix}$, where the structure of matrix $N^{(1)}$ is alike the case of AC/DC/AC converter, and the null-matrix has a size of (8×3). Furthermore, $U_{abc} = U_{abc}^{(1)}$, $I_{abc} = I_{abc}^{(1)}$, $I_{dq} = I_{dq}^{(1)}$, $U_{dq} = U_{dq}^{(1)}$, where $U_{abc}^{(1)}$, $I_{abc}^{(1)}$ are the vectors of phase voltages and currents, respectively, in the node of SMPS connection; $I_{dq}^{(1)}$, $U_{dq}^{(1)}$ are the vectors of images of phase currents and phase voltages, respectively, in the *dq*0 co-ordinate system. Transition matrix $C_{dq} = C_p$, where C_p is the Park's transformation operator.

The main state scale of B_1 is formed according to the algorithm, given by (31). For the SMPS model, however, the number of the state scale element, $i = 1,2,3,4$. Here, $\Lambda_{S_5}^{(1)} = 1$, since there is element $C_5^{(1)}$ in the 5^{th} edge of the graph of *B*-element B_1. According to the operation principles of switching elements included in the edges of the B_2 graph, the main state scale for B_2 is formed with the algorithm provided in (32):

$$\begin{cases} \Lambda_{S_1}^{(2)} = f_S(t),\ \Lambda_{S_2}^{(2)} = 1, \\ \Lambda_{S_3}^{(2)} = \begin{cases} 1, & if\ \Lambda_{S_1}^{(2)} = 0 \\ 0, & if\ \Lambda_{S_1}^{(2)} = 1 \end{cases},\ \Lambda_{S_4}^{(2)} = \begin{cases} 1, & if\ U_{S_4}^{(2)} > 0 \\ 0, & if\ I_{S_4}^{(2)} \le 0 \end{cases}, \\ \Lambda_{S_5}^{(2)} = 0,\ \Lambda_{S_6}^{(2)} = 0,\ \Lambda_{S_7}^{(2)} = 0 \end{cases} \tag{32}$$

where $\Lambda_{S_1}^{(2)}$ is an element of the state scale corresponding to the edge that includes the MOSFET; $f_S(t)$ is the logic function of time supplying the switching function for the MOSFET; element $\Lambda_{S_2}^{(2)}$ corresponds to the edge that includes the SMPS load referred to the primary winding of the SMPS transformer (this edge is always conducting); $\Lambda_{S_3}^{(2)}$ corresponds to the damping circuit of the MOSFET (this edge is conducting, when the edge corresponding to the MOSFET is non-conducting, and vice versa); $\Lambda_{S_4}^{(2)}$ corresponds to the edge including the damping circuit of the load and the diode (the state of this edge depends on the diode state, i.e. conducting or non-conducting), whereas state-scale elements $\Lambda_{S_5}^{(2)}$, $\Lambda_{S_6}^{(2)}$, and $\Lambda_{S_7}^{(2)}$ correspond to the edges designed for voltage measurement respectively on the MOSFET (this edge is always non-conducting), on the load (this edge is always non-conducting) and on the output of the single-phase diode rectifier (this edge is always non-conducting).

4.6 Numerical results

The mathematical model of the integrated active filter is investigated by means of two numerical tests. The task of the first test is to show that the SMPS and the AC/DC/AC converter produce significant conducted emissions in WPS powered from the synchronous generator having a small power.

For demonstration purposes the SMPS is not equipped with an input filter, to simulate the situation when high frequency emissions from a non-linear load are present in the power line. The task of the second test is to check efficiency of the integrated active filter to ensure an appropriate power quality and EMC in the WPS.

Let us first introduce the parameters of the WPS presented in Fig. 1. The power system includes a synchronous generator with nominal power of 1 kW, nominal voltage of 220 V and fundamental frequency of 60 Hz. Parameters of generator are provided in (Belov et. al., 2009).

Harmonic filter 1 is a symmetrical three-phase harmonic filter consisting of three resonant sections tuned to 5th, 7th, 11th harmonics and a parallel capacitor in each electric phase. RLC parameters of the section containing the parallel capacitor are (0.07 Ω, 2.86 μH, 4.5 μF). RLC parameters of the resonant sections are (2.68 Ω, 184.45 mH, 1.26 μF) for resonance frequency 300 Hz, (3.12 Ω, 195.08 mH, 0.74 μF) for resonance frequency 420 Hz, and (16.02 Ω, 24.68 mH, 2.36 μF) for resonance frequency 660 Hz.

A diode rectifier bridge is taken as the rectifier. The diode parameters are the same for all the diodes: $R_{S_1}^{(2)}$ =...= $R_{S_6}^{(2)}$ = 1 mΩ, $L_{S_1}^{(2)}$ =...= $L_{S_6}^{(2)}$ = 5.26 mH. Inductance of the output choke of the rectifier is $L_{S_1}^{(X)}$ = 44.4 mH.

The single-phase inverter has the following parameters: the capacitor acting as the battery, $C_5^{(1)}$ = 1000 μF; equivalent parameters of the switching elements: $R_{S_1}^{(1)}$ =...= $R_{S_4}^{(1)}$ = 10 μΩ, $L_{S_1}^{(1)}$ =...= $L_{S_4}^{(1)}$ = 9.86761 μH. Parameters of the output Γ-filter are L = 1 mH, and C = 30 μF. Threshold level U_H in the inverter control system is taken to be 4 mV.

An electronic product with a 0.075 kW SMPS having the switching frequency 25 kHz is considered. Such a circuit is provided in (Gottlieb, 1994) (Verhees, 2003).

Results of numerical testing of the mathematical model are provided in Fig. 7 and Fig. 8, where symbols "1" and "2"correspond to the first test and to the second test, respectively.

Analysis of the diagrams reveals high efficiency of the integrated active filter.

The first test resulted in the total harmonic distortion (THD) of voltage on the generator terminals to be THD = 0,069956. In the second test the result was THD = 0,00199. Here a complex effect of the active filter on the conducted emissions in the power network has to be noticed. Conducted emissions both from the SMPS and from the voltage inverter of the AC/DC/AC converter are suppressed. As can be seen in Fig. 8, the higher order harmonics almost disappeared after filtering (white bars). In addition, the weight and the dimensions of the equipment enabling the high frequency channel of the voltage inverter are much less than those of harmonic filter 2 designed for the WPS shown in Fig. 1.

5. Conclusion

The methods and models for computer aided design of wind power systems for electromagnetic compatibility and power quality presented in this chapter can be summarized as follows.

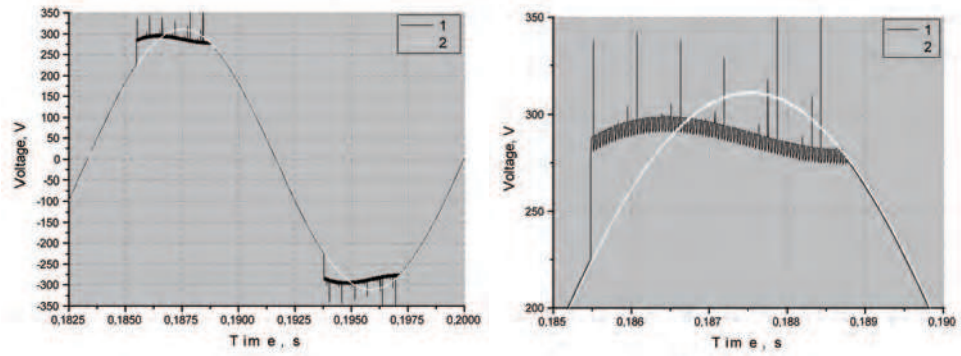

Fig. 7. Voltage diagrams in the SMPS input obtained in tests 1 and 2: the time interval between 0.1825 s and 0.2 s (left) and between 0.185 s and 0.19 s (right).

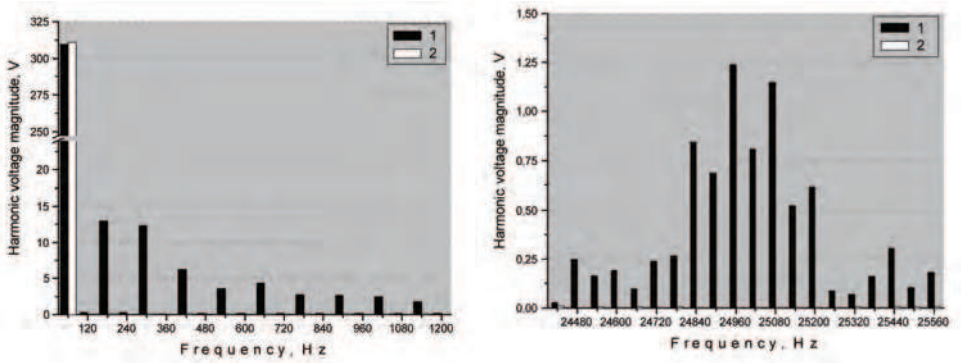

Fig. 8. Voltage spectra in the SMPS input obtained in tests 1 and 2: low frequencies (left) and high frequencies (right).

The iterative spectral technique for power quality and EMC design takes into account changes in the wind power system frequency response during the design procedure. In general, the proposed technique is independent of the circuit of the designed filters. It can be used for designing passive, active and hybrid filters. Further development and generalization of this technique will enable creating universal CAD tools for robust system design.

The multi-phase bridge-element concept for modelling of independent electric power systems with complex power conversion schemes does fully describe the features of wind power systems with AC/DC/AC converter and an SMPS taken as a load. This concept leads to the compact form of the mathematical model of the wind power system represented by the system of ordinary differential equations based on the algebraic calculations and the special algorithm. The algorithm for determining the coefficients of the differential equations enables realization of the PWM technique in the models of control systems for wind power system elements.

The mathematical model of the active power filter integrated into the voltage inverter was derived using the B-element concept. In a wind power system including an AC/DC/AC converter, it is both technically and economically rational to use integrated active filters based on pulse-width modulation. When designing such a filter a very precise choice of parameters is required for the high frequency channel of the voltage inverter control system, which can only be achieved by using the complete mathematical model of the whole power system.

A mathematical model of a multi-phase synchronous generator was introduced as well as a model of a multi-phase ac-load. The system's elements were integrated into the complete model of a multi-phase electric power supply system. This was achieved both by presenting all element models in the canonical form in dq0 coordinate system and by means of the equations for multi-phase power transmission line.

The computational experiments demonstrated the efficiency of the developed mathematical model in designing of the power quality and EMC in the wind power system.

Results of the presented theoretical study and computational experiments supported by the results published earlier by the authors set a framework for computer-aided design of wind power systems with specified power quality and levels of conducted emissions.

The developed methods and models for computer aided design of wind power systems provide a full set of tools for the specialists working with variant design of wind power systems for EMC and power quality, in early design phase. In particular, the developed multi-phase bridge-element concept enables formalization of complex procedures of mathematical modelling multi-cascade circuits of active filters.

The reported iterative spectral technique along with the standard form of models of wind power system elements, based on the multi-phase bridge-element concept and dq0 rotating coordinate system, enable conditions for developing both a user interface and a set of mathematical models for computer aided design tools in the area of wind power system design.

Further theoretical work on developing computer aided design tools for power quality and EMC design could be done in the following areas:

- Realization of fast numerical integration methods for systems of ordinary differential equations.

- Extension of the set of mathematical models via implementation of standard forms of equations for asynchronous motors, DC drives, and various electro-mechanical devices.
- Development of formal criteria for more efficient decision making during the variant analysis within the iterative spectral technique.

6. References

Belov, V. (1993). *Computer-aided EMC Design for Autonomous Power Conversion Systems*, Mordovian State University Press, Saransk (in Russian)

Belov, V. (1998). Mathematical simulation of multiphase electric converting systems, *Journal of Math Modelling*, Vol. 10, No. 10, (1998), 51-63 (in Russian)

Belov, V.; Belov, I.; Nemoykin, V.; Johansson, A. & Leisner, P. (2004) Computer modelling and analysis of EMC in a multi-phase electrical system, *Proceedings of the 3rd national conference on computational electromagnetics - EMB04*, 294-301, Göteborg, Sweden, October 2004

Belov, V.; Paldyaev, N.; Shamaev, A.; Johansson, A.; Leisner, P. & Belov, I. (2005). A complete mathematical model of an independent multi-phase power supply system based on multi-phase bridge-element concept, *WSEAS Transactions on Circuits and Systems*, Vol. 4, No. 9, (September 2005), 1009-1018

Belov, V.; Shamaev, A.; Leisner, P.; Johansson, A.; Magnhagen, B. & Belov, I. (2006). A simulation-based spectral technique for power quality and EMC design of an independent power system, *International Journal of Emerging Electric Power Systems*, Vol. 7, No. 1, (2006), Article 7

Belov, V.; Leisner, P.; Johansson, A.; Paldyaev, N.; Shamaev, A. & Belov, I. (2009) Mathematical modelling of a wind power system with an integrated active filter, *Journal of Electric Power Systems Research,* Vol. 79, No. 1, (2009), 117-125

Binsaroor, A. & Tiwari, S. (1988). Evaluation of twelve phase (multiphase) transmission line parameters, *Journal of Electric Power Systems Research*, Vol. 15, (1988), 63-76.

Brown, D. & Chandrasekaran, B. (1989). *Design Problem Solving: Knowledge Structures and Control Strategies*, Morgan Kaufmann, Los Altos, CA

EMC Filters Data Book, (2001). EPCOS AG Marketing Communications, Munich

Gottlieb, I. (1994). *Power Supplies, Switching Regulators, Invertors, and Converters*, TAB Books, Division of Mc Draw-Hill, New York

Grauers, A. (1994). *Synchronous Generator and Frequency Converter in Wind Turbine Applications: System Design and Efficiency*, *Lic. thesis*, *Technical Report No. 175L* Chalmers University of Technology, ISBN 91-7032-968-0, Göteborg, Sweden

Himmelblau, D. (1972). *Applied Nonlinear Programming*, McGraw-Hill, New York.

Ortuzar, M. ; Carmi, R. ; Dixon, J. & Morán, L. (2003) Voltage source active power filter, based on multi-stage converter and ultracapacitor DClink, *Proceedings of IEEE industrial electronics conference - IECON'2003*, 2300 – 2305, Roanoke, Virginia, USA, November 2003

Park, R. (1929). Two-reaction theory of synchronous machines - part 1, *AIEE Transactions*, Vol. 48, (1929), 716-730

Temes, G.; Mitra, S. (1973) *Modern Filter Theory and Design*, John Willey & Sons, 1973

Toliyat, H.; Shi, R. & Xu, H. (2000) A DSP-based vector control of five-phase synchronous reluctance motor, *Proceedings of the IEEE-IAS 2000 annual meeting*, 1759-1765, Rome, Italy, October 2000

Verhees, H. (2003). *TEA1541 SMPS Control IC with Synchronization Function*, *AN10205-01*, Philips Electronics N.V.

Wind Power

Edited by S M Muyeen

ISBN 978-953-7619-81-7
Hard cover, 558 pages
Publisher InTech
Published online 01, June, 2010
Published in print edition June, 2010

This book is the result of inspirations and contributions from many researchers of different fields. A wide verity of research results are merged together to make this book useful for students and researchers who will take contribution for further development of the existing technology. I hope you will enjoy the book, so that my effort to bringing it together for you will be successful. In my capacity, as the Editor of this book, I would like to thanks and appreciate the chapter authors, who ensured the quality of the material as well as submitting their best works. Most of the results presented in to the book have already been published on international journals and appreciated in many international conferences.

How to reference

In order to correctly reference this scholarly work, feel free to copy and paste the following:

Vladimir Belov, Peter Leisner, Nikolay Paldyaev, Alexey Shamaev and Ilja Belov (2010). Methods and Models for Computer Aided Design of Wind Power Systems for EMC and Power Quality, Wind Power, S M Muyeen (Ed.), ISBN: 978-953-7619-81-7, InTech, Available from: http://www.intechopen.com/books/wind-power/methods-and-models-for-computer-aided-design-of-wind-power-systems-for-emc-and-power-quality

INTECH
open science | open minds

InTech Europe
University Campus STeP Ri
Slavka Krautzeka 83/A
51000 Rijeka, Croatia
Phone: +385 (51) 770 447
Fax: +385 (51) 686 166
www.intechopen.com

InTech China
Unit 405, Office Block, Hotel Equatorial Shanghai
No.65, Yan An Road (West), Shanghai, 200040, China
中国上海市延安西路65号上海国际贵都大饭店办公楼405单元
Phone: +86-21-62489820
Fax: +86-21-62489821